Available online at www.sciencedirect.com

SciVerse ScienceDirect

Journal of the European Ceramic Society 32 (2012) 1651–1658

www.elsevier.com/locate/jeurceramsoc

Electrohydrodynamic atomization deposition of PZT sol–gel slurry and sol infiltration on the films

D. Wang [a,*], S.A. Rocks [b], R.A. Dorey [c]

[a] *Key Laboratory for Micro/Nano Technology and System of Liaoning Province, Dalian University of Technology, Dalian, Liaoning Province, 116024, China*
[b] *Collaborative Centre of Excellence in Understanding and Managing Natural and Environmental Risks, Cranfield University, Bedfordshire MK43 0AL, UK*
[c] *Microsystems & Nanotechnology Centre, Cranfield University, Bedfordshire MK43 0AL, UK*

Received 12 June 2011; received in revised form 24 November 2011; accepted 11 December 2011
Available online 17 January 2012

Abstract

This paper reports the use of a deposition technique, called electrohydrodynamic atomization, for producing PZT films from a composite sol–gel slurry. PZT slurries of different powder concentrations were prepared, and then atomization deposition of them was carried out and resultant films examined. It was observed that large splats with well-mixed PZT particles in sol and fine PZT clusters with dry PZT particle agglomeration can be deposited using this technique. In particular, intermediated sol infiltration process on the EHDA deposited film under optimized atomization condition was also studied. It was found that the film with sol infiltration process become more dense and the electrical properties (P_r, ε_r) were improved compared with that without sol infiltration after EHDA deposition.

Keywords: A. Films; A. Suspensions; C. Ferroelectric properties; D. PZT; Electrohydrodynamic atomization

1. Introduction

Lead zirconate titanate (PZT) is a versatile material because of the combination of its ferroelectric, piezoelectric, dielectric and pyroelectric properties and excellent performance. Recently PZT has been widely used in non-volatile memory applications[1] and micro-electromechanical system (MEMS).[2–4] PZT films with different thickness ranges are needed for different applications.[5–8] However, the deposition of PZT thick films (10–100 μm) is still a challenge. The machining of bulk PZT ceramics to fabricate these films presents difficulty in the slicing and handling of thin and fragile ceramic components. Thin film fabrication methods, such as physical vapour deposition and chemical vapour deposition, are associated with slow deposition rates and high levels of stress generated during processing, which can lead to cracking when forming thick films.[9] Techniques based on the sintering of ceramic particles, such as screen printing, are limited by high temperature processing which commonly result in damage to electrodes and substrate.[10] Wet chemical methods, such as sol–gel, allow a low sintering temperature (600 °C) process, but are limited to a maximum thickness of around 3 μm.[11] Through using spin-coating techniques and composite PZT sol–gel slurry, it is possible to fabricate 35 μm thick PZT films at relative lower sintering temperature (∼720 °C); however, it is still time-consuming and is likely to induce excess stresses which can cause curvature of substrate.[12]

Electrohydrodynamic atomization (EHDA) is a physical process, where a liquid jet breaks up into droplets due to electric and mechanical forces,[13] which was first reported by Zeleny in 1914.[14] The atomizer nozzle is a metal capillary into which liquid or suspension can be pumped. When a high voltage is applied between the nozzle and base electrode, shear stress on the liquid surface is generated which causes elongation of a jet and its disintegration into droplets. Droplets of a few nanometres in size with narrow size distribution can be obtained by this method.[15] Depending on the conditions (including electric field, liquid flow rate, geometry of nozzle dimension and liquid properties) different modes can be formed such as dripping, microdripping, spindle, multi-spindle, cone-jet and multi-jet.[16]

* Corresponding author. Tel.: +86 41184707713; fax: +86 41184707940.
E-mail address: d.wang@dlut.edu.cn (D. Wang).

0955-2219/$ – see front matter © 2012 Elsevier Ltd. All rights reserved.
doi:10.1016/j.jeurceramsoc.2011.12.013

Since the 1990s, ceramic suspensions has been subjected to this process to form microstructures in bioengineering[17] and chemical engineering.[18]

Composite PZT powder/sol slurries were prepared and used in EHDA technique in this work for their low sintering temperature and the possibility of making films with thicknesses ranging from micrometers to millimetres.[19] The integration of the composite PZT powder/sol slurry and EHDA technique provides a new deposition method with great advantage of fast speed, convenience, and low cost. In particular, a relatively large needle (>200 μm) can be used in EHDA to form fine droplets,[20] which significantly reduces the risk of needle blockage during deposition that often happens in ink-jet printing. This method has great potential as a commercial fabrication method in MEMS manufacture.

In our previous work EHDA combined with a micromoulding technique was used to form PZT ceramic micro-scale structures with the advantages of avoiding the use of hazardous solutions used in chemical wet etching process and low sintering temperature. However, the fabricated PZT thick film structures still presented porous feature and relatively low electrical properties.[21] In this work composite PZT sol–gel slurries with different powder loadings were deposited using the EHDA technique, and statistic and structural analyses of the deposited films were carried out. Moreover, PZT sol infiltration of the deposited PZT film was also conducted to improve the density and electrical properties of the films.

2. Experimental details

2.1. PZT sol

Two types of PZT sol were used in this work, one was prepared based on propanol solvent, another one was prepared using 2-methoxyethanol (2-ME) as the solvent. The propanol based PZT sol was mixed with PZT powder in order to make the PZT slurry for the EHDA deposition process. The 2-ME based PZT sol was used for the intermediated infiltration of the PZT films produced by the EHDA deposition. The 2-ME based sol has previously been shown result in films with high properties but is unsuitable for spray deposition due to the hazards associated with it. For this reason the 2-ME sol was only used for infiltration processes in order to maximise the properties of the films.

The propanol based PZT sol was prepared from the precursors lead (II) acetate trihydrate, titanium (IV) isopropoxide and zirconium (IV) propoxide. Titanium (IV) isopropoxide (99.99 wt.% purity, 3.55 g) was mixed with zirconium (IV) propoxide (76 wt.% in 1-propanol, 5.39 g) prior to the addition of the solvents 1-propanol (99.7 wt.% purity, 5 ml) and glacial acetic acid (99.8 wt.% purity, 10 ml). An excess of lead (II) acetate trihydrate (9.95 g) was then added to the solution and the system was refluxed at 95 °C for 30 min. The sol concentration was adjusted to 0.6 M by adding 11 ml 1-propanol and 10 ml acetic acid. This PZT sol exhibited a perovskite structure when crystallised at 650 °C.[22] The 2-ME based PZT sol was prepared from the precursors lead (II) acetate trihydrate, titanium (IV) isopropoxide, zirconium (IV) propoxide, niobium (V) ethoxide, antimony (III) ethoxide and manganese (II) acetate. The preparation process of the 2-ME based PZT sol was described in our previous work,[23] and the concentration obtained was 1.1 M. The composition of the 2-ME based PZT organometallic solution was precisely matched to the PZT powder (PZ26) used for making PZT slurry. After preparation the sols were stored in a glass desiccators chamber under vacuum. The propanol based PZT sol was used to make PZT slurry soon after preparation, and the 2-ME based PZT sol was used for the films infiltration within 5 days of the sol prepared. As pure sol systems, both sols have shelf lives in excess of 1 month.

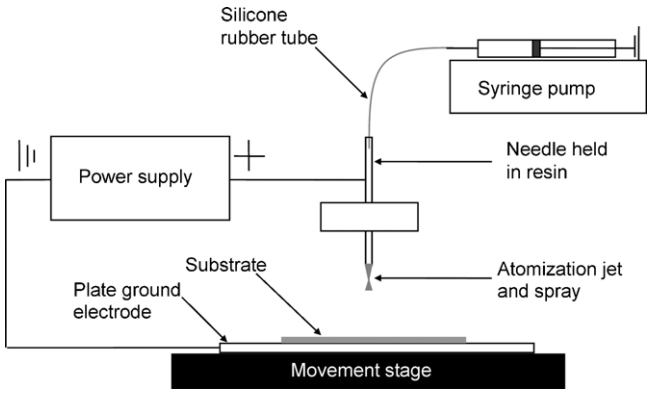

Fig. 1. Schematic diagram of EHDA deposition equipment set-up.

2.2. PZT slurry

The PZT slurry was prepared by mixing PZT powder (PZ26, Ferroperm, Denmark), propanol based PZT sol, sintering aid of CuO_2–PbO, dispersant KR55 (Ken-React Lica 38, KenRich) and solvent of 1-propanol and acetic acid in a nitrogen environment, then ball-milled for 24 h. The PZT power (PZ26) is a hard doped PZT composition with a mean particle size of ~0.6 μm and a chemical composition of $Pb_{1.1}[Nb_{0.02}Sb_{0.02}Mn_{0.02}(Ti_{0.48}Zr_{0.52})_{0.94}]O_3$. The PZT slurry was stored in a glass desiccator under vacuum after preparation and was used for EHDA deposition within 5 days of production.

In the PZT film the sol derived material acts as a network between the PZT particles to glue and bind them together, and also reduces the sintering temperature and hence decreases lead volatilisation.[24,25] The sintering aid can help to increase the density and piezoelectric properties of the PZT film formed.[23] The components and different contents of PZT slurry are shown in Table 1. The addition of sintering aid CuO_2–PbO and dispersant KR55 was kept at 0.069/0.428 g and 0.2 g for all the PZT slurry mixtures prepared. The PZT powder and propanol based PZT sol ratio was kept at 10 g to 10 ml, and the additional solvent made of 1-propanol and acetic acid (with the volume ratio of 1.1:1) was varied from 0 ml to 8.4 ml. The PZT slurry was ball-milled again for 2 h immediately before use.

2.3. Deposition of PZT slurry and sol infiltration on the film

The EHDA deposition device is shown in Fig. 1, which consists of the electrohydrodynamic spray nozzle coupled together

Table 1
The composition of PZT slurries and the relevant EHDA working parameters.

Powder/sol/1-propanol/acetic acid	PZT powder (g)	PZT sol (ml)	Solvent		Flow rate (10^{-10} m^3 s^{-1})	Applied voltage (kV)
			1-Propanol (ml)	Acetic acid (ml)		
10–10–0–0	10	10	0	0	3.9	7.5
10–10–0.55–0.5	10	10	0.55	0.5	3.6	7.5
10–10–1.1–1	10	10	1.1	1	3.1	7.5
10–10–2.2–2	10	10	2.2	2	2.2	7.5
10–10–3.3–3	10	10	3.3	3	1.7	7.5
10–10–4.4–4	10	10	4.4	4	1.1	7.5

with a computer controlled *X–Y* movement stage. The needle (inner/outer diameter of 0.85/1.3 mm) was connected to a high voltage power supply (Glassman High Voltage Inc., NJ, USA), which was used to provide an electric field between the needle and the ground electrode. The inlet of the needle was connected to a syringe pump (KD Scientific Inc., MA, USA) using a silicone rubber tube, which was employed to provide the hydrodynamic force to push the PZT slurry to the outlet of the needle. A thin aluminium plate, serving as the ground electrode, was placed directly on the *X–Y* movement stage and connected to earth potential.

A 2.5 cm × 2.5 cm silicon wafer substrate coated with sputtered Ti/Pt (8/100 nm) was placed on the aluminium plate ground electrode and kept at a fixed distance from the needle throughout deposition. In order to allow the effect of solvent addition on droplet distribution to be examined a single quick pass deposition was carried out with a stage speed of 30 mm/s. In order to deposit a film over a large area, and to study the resultant film, a raster pattern was used alternating between one layer with the long path in the *X* direct (step in *Y* direction) and the next with the long path in the *Y* direction (step in the *X* direction). The travelling speed was 30 mm/s, and the distance between two parallel paths of deposition was set to 3.6 mm to ensure a degree of overlap between deposited material.[26] After every two layers of EHDA deposition the PZT film was dried at 200 °C for 60 s and pyrolysed at 350 °C for 60 s using a hotplate to remove organic components. In order to increase the density of the films, after every 20 layers of EHDA deposition the film was infiltrated three times with a 2-ME based PZT sol using spin coating technique (2000 rpm for 30 s). The same heating process was applied to each PZT sol infiltration treatment before the subsequent infiltration process was conducted. The completed film was sintered at 720 °C for 20 min in muffle furnace. In order to examine the electrical properties of the PZT films a chromium/gold top electrode with a thickness of 15/100 nm and a diameter of 770 μm was deposited using a vacuum evaporation (Edwards Evaporator E480, Crawley, UK) on the PZT film surface after sintering.

3. Results and discussion

3.1. Deposition of PZT slurry with solvent variation

Representative results of a single deposition pass, are shown in Fig. 2. During the deposition, the working distance between the needle outlet and the substrate was set at 2 cm, in order to obtain stable atomization jet at the outlet of the needle, and the applied voltage was kept at 7.5 kV. The deposition was carried out for all PZT slurry mixtures detailed in Table 1 with deposition parameters as stated. The deposition product was shown to be a combination of large flattened circular deposits (splats) and small spherical clusters (Fig. 2d). Splats contain well-mixed PZT powder in sol, and clusters are hard PZT particle agglomerations. The size of splats and clusters and their corresponding number were measured and counted from the SEM micrographs obtained. The analysis of the deposition results is summarized in Table 2. The influence of the additional solvent on the size and number density of the splats is shown in Fig. 3. The addition of extra solvent to the system has two effects. Firstly, it caused a reduction in the concentration of the sol phase acting as the carrier fluid. Secondly, it results in a reduction in the powder loading in the slurry.

At low solvent additions larger sized (∼70 μm) and a lower number density (∼30 number/mm^2) of splats were produced (Fig. 3). In addition cracks were evident in the film after one layer deposition (Fig. 2a) due to the high shrinkage induced stress in the large volume splats during the drying process. As more solvent was added, the observed cracks were smaller (Fig. 2b and c) probably due to the reduction of the size of splats (Table 2) and the subsequent reduction in stress generated during the drying procedure. No cracks were evident when 4.2 ml of solvent was added (Fig. 2d), and the greatest frequency of deposited splats was noted at this dilution (Fig. 3). With still further additions of solvent (6.3 ml and 8.4 ml of solvent addition), the slurry produced even smaller size splats, and clusters became the dominant features (Fig. 2e and f). Two factors caused the reduction in the size of the splats when more solvent was added to the slurry: (1) the lower flow rate needed to form a stable jet led to a reduction in the jet diameter and size of the atomized products; and (2) the higher solvent volume content in the slurry led to greater percentage drop size reduction during flight as solvent evaporated. These two factors combined – smaller drops produced, and greater (and faster) evaporation – resulted in a case where increased electrostatic induced breakup of individual drops occurred during the EHDA process resulting in the formation of smaller relics that manifested as clusters. Electrostatic breakup occurs when the charged droplet decreases in size to a critical value where surface tension is overcome due to charge.

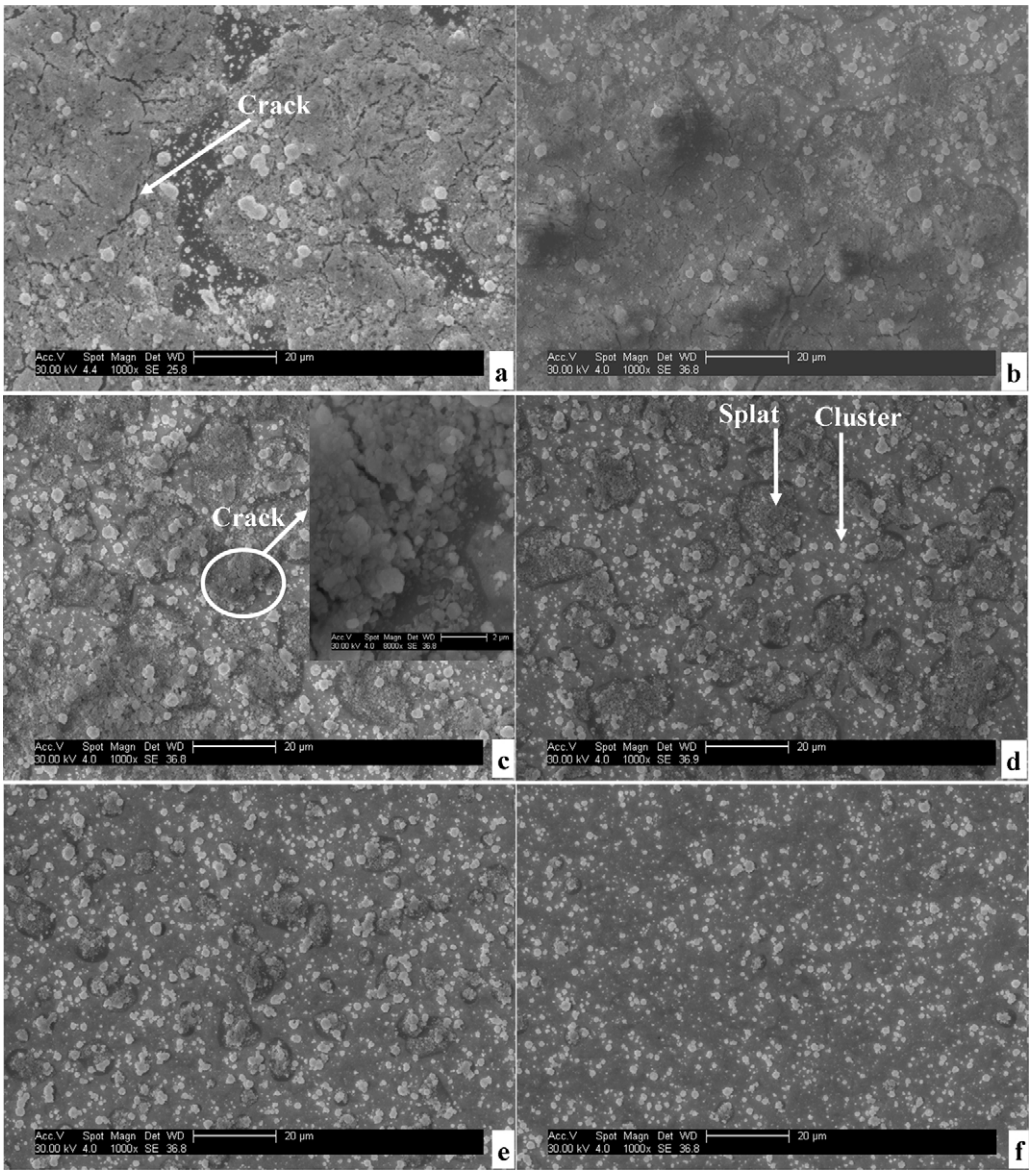

Fig. 2. Scanning electron microscope micrographs showing the one layer deposition of PZT slurry at an applied voltage of 7.5 kV and different flow rates and solvent additions (a) 3.9×10^{-10} m^3 s^{-1} and 0 ml, (b) 3.6×10^{-10} m^3 s^{-1} and 1.05 ml, (c) 3.1×10^{-10} m^3 s^{-1} and 2.1 ml, (d) 2.2×10^{-10} m^3 s^{-1} and 4.2 ml, (e) 1.7×10^{-10} m^3 s^{-1} and 6.3 ml and (f) 1.1×10^{-10} m^3 s^{-1} and 8.4 ml.

The size of the clusters produced showed a slight, but statistically insignificant, increase in size with the addition of solvent to the slurry (Fig. 4). The number density of clusters decreased slightly with the increases in solvent addition most likely due to the decreased flow rates required to achieve stable atomization as the solvent volume is increased.

Given the average size (0.6 μm) of the PZT particles used in the slurry and the size of the clusters observed (0.3–3 μm) it is

Table 2
Statistic analysis of splats and clusters deposited from different PZT slurry composition.

Powder/sol/1-propanol/acetic acid	Splat				Cluster			
	Min. (μm)	Max. (μm)	Aver. (μm)	Std. dev.	Min. (μm)	Max. (μm)	Aver. (μm)	Std. dev
10–10–0–0	56.9	78.4	67.7	15.1	0.3	3.0	0.7	0.5
10–10–0.55–0.5	6.0	27.4	18.1	6.2	0.3	3.0	0.7	0.5
10–10–1.1–1	5.1	25.3	12.1	5.5	0.3	3.0	0.7	0.5
10–10–2.2–2	2.9	19.5	7.9	3.4	0.3	3.0	0.7	0.5
10–10–3.3–3	2.8	10.9	6.0	2.0	0.3	3.0	0.8	0.6
10–10–4.4–4	2.8	5.3	3.7	1.0	0.3	3.0	0.8	0.5

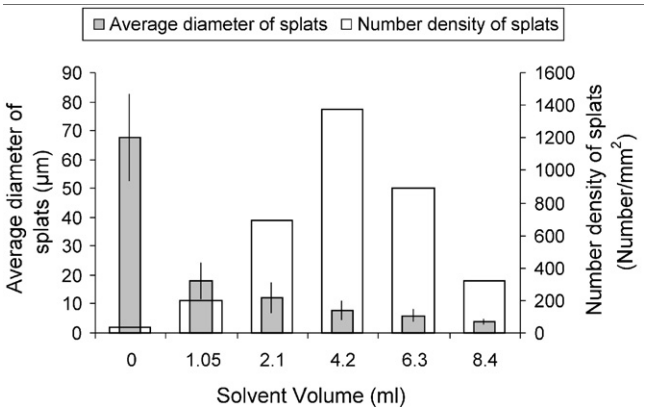

Fig. 3. Influence of solvent volume on splat size and density for EHDA deposited sol–gel systems based on 10 g PZT powder, 10 ml PZT sol and solvent of 0, 1.05, 2.1, 4.2, 6.3 and 8.4 ml.

reasonable to assume that the clusters are typically composed of less than 10 particles. For such clusters to have been created purely through the evaporation of solvents from individual droplets (without electrostatic breakup) the originating droplets would have to have radii close to 2 μm. Droplets of such size are not likely to have been produced by the experimental apparatus used in this work and if produced would tend to discount the production of droplets of sufficient size required to produce the splats observed. Such an observation lends further evidence to the electrostatically induced breakup of the drying drops during flight.

3.2. Deposition of PZT film and the effect of sol infiltration

Based on the deposition characteristics shown in single pass analysis, it is proposed that splats are required for the formation of a high density PZT film using the EHDA technique as the liquid nature of the droplets will allow particle rearrangement to occur on deposition. The ideal deposition parameters for EHDA film formation would be the parameters that result in a high number density of large splats without cracks. With the above analysis, the slurry that produced a crack-free

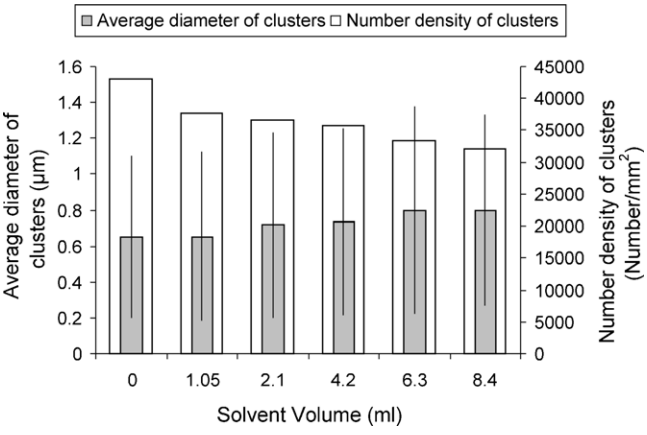

Fig. 4. Influence of solvent volume on cluster size and density for EHDA deposited sol–gel systems based on 10 g PZT powder, 10 ml PZT sol and solvent of 0, 1.05, 2.1, 4.2, 6.3 and 8.4 ml.

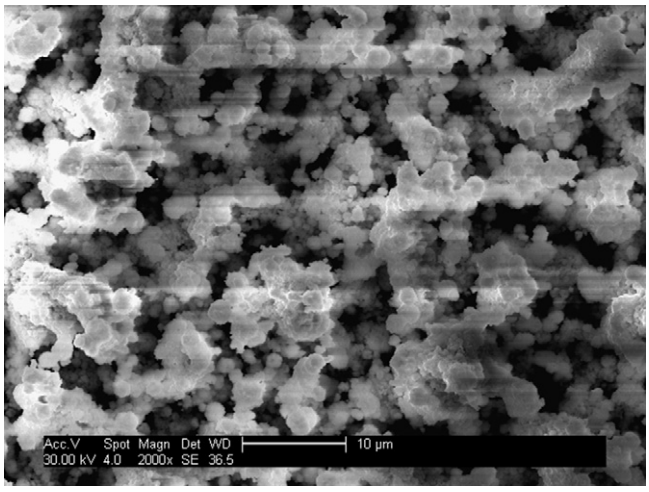

Fig. 5. Scanning electron microscope micrographs showing the microstructure of the surface of 20 layer PZT film produced using EHDA deposition at a working distance of 2 cm and solvent addition of 4.2 ml.

deposition (4.2 ml solvent addition) was considered to have the best potential to form dense and crack-free films. Therefore, the PZT slurry with 4.2 ml solvent was used to deposit 20 layers PZT films in this work. The deposition conditions were kept the same as the one layer deposition in the previous section. To avoid sedimentation, fresh slurry was used after 10 layers of EHDA deposition, and the needle was cleaned at that time. The total time to complete 20 layers of deposition was approximately 33 min. Fig. 5 shows the 20 layer films produced from the slurry with 4.2 ml solvent addition, which exhibits a highly porous microstructure. This is mainly caused by the small size of splats deposited (Fig. 2d) which are not big enough to cover a large area to form a dense film. Moreover, the clusters deposited can serve as an electrode for the other incoming clusters and thus attracting them to preferential sites, resulting in the porous microstructure observed.[22]

It was observed from the above analysis that although numerous crack-free splats can be produced using the PZT slurry with 4.2 ml solvent, their small size and tendency for selective deposition can cause the formation of pores. In order to mitigate this the working distance between needle and substrate was reduced to 1 cm. The smaller working distance helps to reduce droplet break-up and lessen solvent evaporation during their shorter travelling time from needle exit to substrate, which can help to overlap the droplet with well-mixed PZT particles deposited between successive layers during the EHDA deposition process and lead to the formation of dense films. During this study three typical slurries were used to deposit 60 layers PZT films: (1) slurry with the highest sol concentration (no additional solvent), (2) slurry with crack-free deposition product (4.2 ml solvent) and (3) slurry with even lower sol concentration (6.3 ml solvent addition). The flow rate was not varied from that used for the 2 cm working distance deposition, but the applied voltage was changed to 5.5 kV in order to obtain a stable EHDA jet.

Firstly, the slurry with highest PZT sol concentration was used to deposit 60 layer films (Fig. 6a). Large cracks are

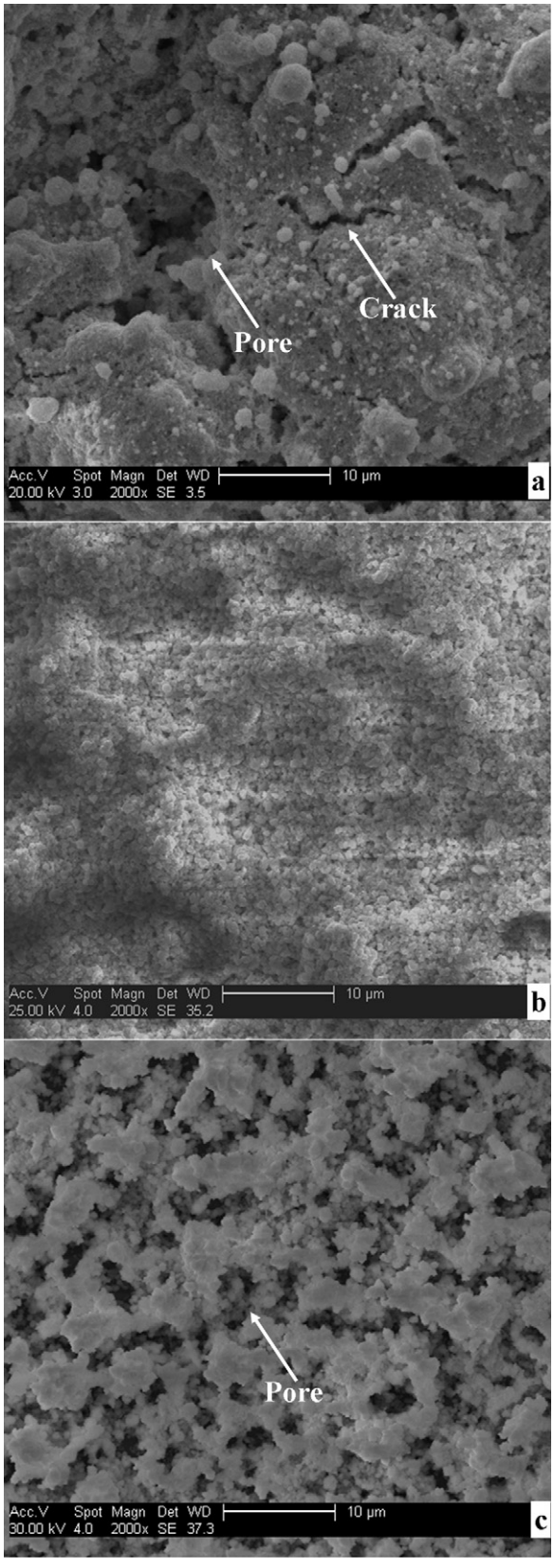

Fig. 6. Scanning electron microscope micrographs showing the microstructure of the surface of 60 layer PZT film produced using EHDA deposition at a working distance of 1 cm, an applied voltage of 5.5 kV and different flow rates and solvent additions (a) 3.9×10^{-10} m^3 s^{-1} and 0 ml, (b) 2.2×10^{-10} m^3 s^{-1} and 4.2 ml and (c) 1.7×10^{-10} m^3 s^{-1} and 6.3 ml.

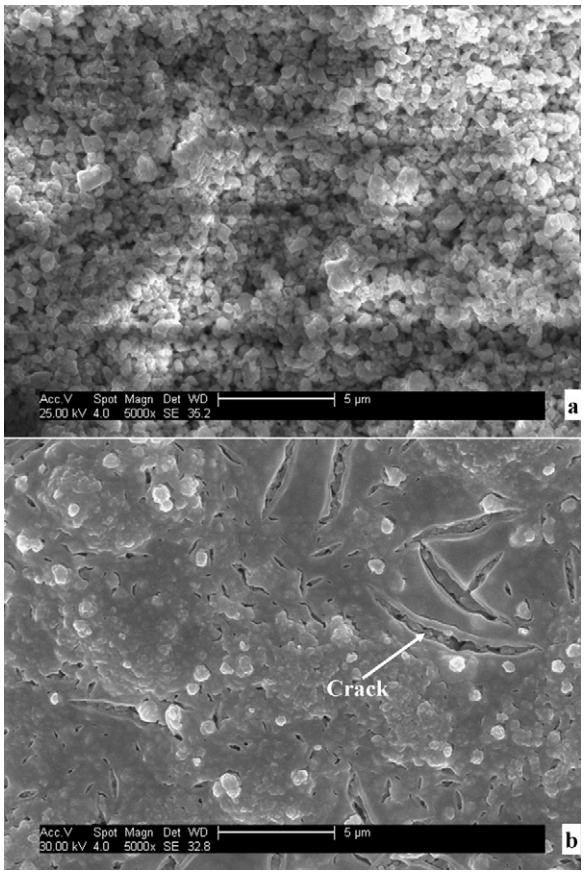

Fig. 7. Scanning electron microscope micrographs showing the microstructure of the surface of the PZT films without (a) and with (b) sol infiltration process.

evidenced in the film, which can be predicted from the one layer deposition results containing large splats with cracks after drying (Fig. 2a). Pores are also observed in the film, which is due to the co-location of uncovered areas between successive layers during the EHDA deposition process. 60 layer films produced from the slurry with 4.2 ml solvent addition is shown in Fig. 6b, which is characterised by well-packed PZT particles in the films with crack-free features. This feature shows the well-organized splats (big enough and high number density) overlapped between successive layers to form dense and crack-free film. The thickness of this film is about 26 μm, measured using a Surface Profiler (Veeco Instruments Incorporation, UK). Thirdly, PZT slurry with even lower sol concentration (6.3 ml solvent addition) was used to form 60 layer films (Fig. 6c), which presented a porous and powdery surface. This was caused by the even smaller and lower number density of splats and the dominance of dry clusters in the deposition products using this slurry (Fig. 2e).

Although the well-packaged and dense PZT thick film was formed using the PZT slurry combined with the EHDA deposition technique, submicron-pores were observed between the PZT particles (Fig. 7a) which are indicative of weakness of the film and can reduce the properties of the film.[27] In order to reduce the level of porosity, intermediate multiple 2-ME based sol infiltration treatments were applied to the EHDA deposited film.

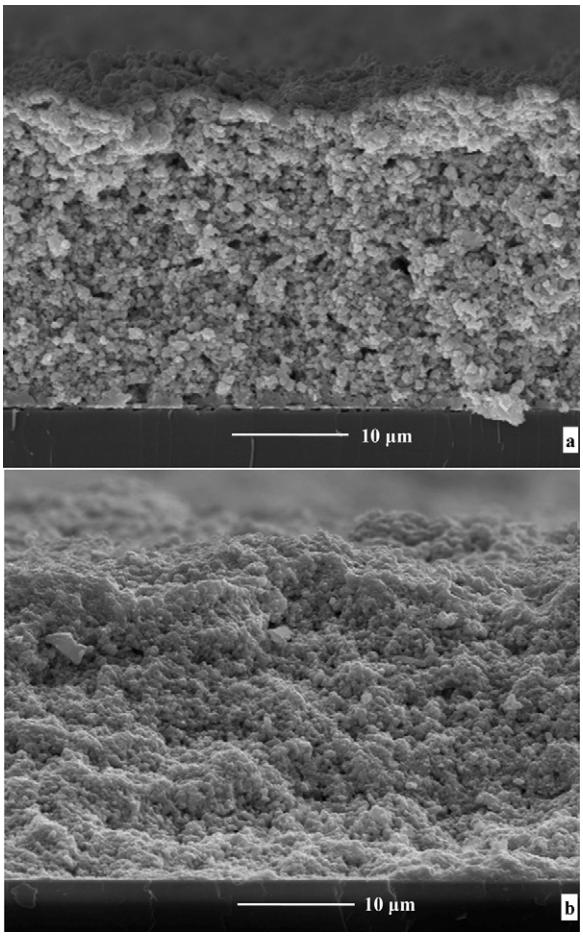

Fig. 8. Scanning electron microscope micrographs showing the microstructure of the cross-section of the PZT films without (a) and with (b) sol infiltration process.

Fig. 7 shows the surface of the PZT film with and without PZT sol infiltration process after 60 layers deposited using EHDA. It can be seen that the submicron-pores between the PZT particles that were present in the EHDA deposited film (Fig. 7a) were filled after three sol infiltration treatments using the spin coating technique (Fig. 7b). This increased the bonding behaviour of the PZT particles and reduced the porosity of the film. It can also be seen that cracks appeared where sol was retained in the concave depressions in the EHDA deposited PZT film following the spin coating process after sol infiltration (Fig. 7b). These cracks extend only through the surface sol layer and are due to the high level of shrinkage induced stress in the sol on drying and pyrolysis.

Fig. 8 shows the cross-section of 60 layer PZT films with and without PZT sol infiltration after every 20 layers. The porosity is ~11% after intermediated multiple sol infiltration process which is slightly lower than that without infiltration (~14%). These porosities were deduced from scanning electron microscopy micrographs of film fracture cross sections. It was observed that the infiltration was complete (Fig. 8b) and that more than 3 treatments at intermediate levels resulted in this pooling of sol–gel material which then begins to degrade properties.

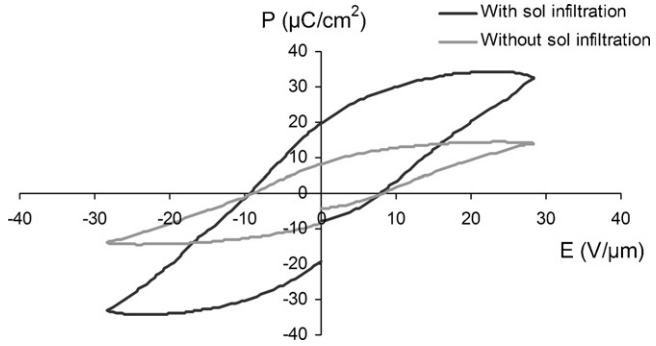

Fig. 9. Ferroelectric hysteresis loop of the PZT films with and without sol infiltration.

3.3. Electrical characterisation

The relative permittivity (ε_r) of the PZT films with sol infiltration process was calculated to be 393 (±8) at 50 kHz and was higher than that without sol infiltration process (260 ± 9), and the dielectric losses were all less than 0.02. These changes are likely to be as a result of the reduction of porosity of the PZT films after sol infiltration. The values of relative permittivity quoted by the manufacturer for PZ26 is 1300 which is greater than that obtained from films made using EHDA deposition process. The reduction in the relative permittivity in the films relative to the bulk is mainly attributed to the presence of residual porosity,[28] different grain sizes and because of the presence of a rigid substrate which reduces the piezoelectric contribution to relative permittivity due to clamping.[29] The values of relative permittivity agree well with those found for other thick films produced by spin coating[19] and screen printing.[30]

It was found that the highest film piezoelectric constant ($d_{33,f}$) of the EHDA deposited films with and without sol infiltration process did not vary greatly, both were around 70 pC/N when poled at 12 V/μm at 200 °C for 5 min. The low variation in d_{33} between infiltrated and non-infiltrated films is mainly due to the dominant effect of the sintering aid addition and the fact that above a critical density additional sol infiltrations do not result in an increase in d_{33}.[23] Bardaine et al. also reported that additional infiltrations can improve the density of PZT films but not piezoelectric performance.[31]

Fig. 9 shows the ferroelectric hysteresis loops of PZT films with and without sol infiltration, which becomes saturated at the electric field intensity of 28 V/μm. Remnant polarization (P_r) of the PZT film after sol infiltration (19.5 μC/cm^2) is approximately double of that without sol infiltration (8.3 μC/cm^2), due to the effects of densification and reduction of pore size.[32] The coercive field has no distinct difference after the sol infiltration process. The $d_{33,}$ ε_r and P_r obtained in this work using EHDA deposition and infiltration process are lower than those of bulk PZT materials, which is mainly due to the existence of residual pores, and different grains sizes in the films as well as the presence of the rigid substrate constraining the film. However, these value are comparable to the composite films at the equal level of thickness produced using the screen printed and spin coating PZT.[30,33]

4. Conclusions

The deposition of PZT slurries using an EHDA technique and intermediate PZT sol infiltration was demonstrated in this paper. The deposition products consist of splats and clusters, the features of which were shown to be affected by the concentration of the sol and powder loading in the slurry during EHDA deposition. Higher sol concentration and powder loading in the slurry led to bigger size and lower number density of splats, whereas lower sol concentration and lower powder loadings resulted in smaller splats and dry clusters. The EHDA deposited PZT film with 2-ME sol infiltration exhibited a higher density than that without sol infiltration, and an increased remnant polarization (P_r) and relative permittivity (ε_r) were also obtained after sol infiltration. The plateau value of piezoelectric coefficient ($d_{33,f}$) of ~70 pC/N was observed with and without sol infiltration on the PZT films. This process demonstrates a promising way for forming PZT thick films with dense and crack-free feature and desirable electrical properties for the requirement of MEMS device fabrication.

Acknowledgements

The authors would like to thank Dr. Christopher Shaw and Mr. Andrew Stallard for their generous help with this work. This work is funded by EPSRC (GR/84156/01), the European commission as part of the MIND (Multifunctional & Integrated Piezoelectric Device) project and the Piezo Institute. Dazhi Wang acknowledges the work supported by the National Natural Science Foundation of China (No. 50905027) and Specialized Research Fund for the Doctoral Program of Higher Education of China (No. 20090041120041).

References

1. Scott JF, Dearaujo CAP. Ferroelectric memories. *Science* 1989;**246**:1400–5.
2. Gebhardt S, Seffner L, Schlenkrich F, Schonecker A. PZT thick films for sensor and actuator applications. *J Eur Ceram Soc* 2007;**27**: 4177–80.
3. Kim H, In C, Yoon G, Kim J. Design and fabrication of a micro PZT cantilever array actuator for applications in fluidic systems. *J Mech Sci Technol* 2005;**19**:1544–53.
4. Zhang QQ, Djuth FT, Zhou QF, Hu CH, Cha JH, Shung KK. High frequency broadband PZT thick film ultrasonic transducers for medical imaging applications. *Ultrasonics* 2006;**44**:E711–5.
5. Xiong S, Kawada H, Yamanaka H, Matsushima T. Piezoelectric properties of PZT films prepared by the sol–gel method and their application in MEMS. *Thin Solid Films* 2008;**516**:5309–12.
6. Polla DL, Schiller PJ. Integrated ferroelectric microelectromechanical systems (MEMS). *Int Ferroelectrics* 1995;**7**:359–70.
7. Xu XH, Chu JR. Preparation of a high-quality PZT thick film with performance comparable to those of bulk materials for applications in MEMS. *J Micromech Microeng* 2008;**18**:65001.
8. Tu YL, Milne SJ. Processing and characterization of Pb(Zr,Ti)O-3 films, up to 10 μm thick, produced from a diol sol–gel route. *J Mater Res* 1996;**11**:2556–64.
9. Zhou QF, Chan HLW, Choy CL. Conducting lanthanum nickel oxide as electrodes for lead zirconate titanate films. *Thin Solid Films* 2000;**375**:95–9.
10. Mass R, Koch M, White NM, Evans AGR. Thick-film printing of PZT onto silicon. *Mater Lett* 1997;**31**:109–12.
11. Ledermann N, Muralt P, Baborowski J, Gentil S, Mukati K, Cantoni M, et al. {1 0 0}-Textured, piezoelectric $Pb(Zr_x,Ti_{1-x})O_3$ thin films for MEMS: integration, deposition and properties. *Sens Actuators A* 2003;**105**:162–70.
12. Dauchy F, Dorey RA. Patterned high frequency thick film MEMS transducer. *Integr Ferroelectr* 2007;**90**:42–52.
13. Jaworek A, Krupa A. Classification of the modes of EHD spraying. *J Aerosol Sci* 1999;**30**:873–93.
14. Zeleny BJ. The electrical discharge from liquid points, and a hydrostatic method of measuring the electric intensity at their surfaces. *Phys Rev* 1914;**3**:69–91.
15. Loscertales IG, Barrero A, Guerrero I, Cortijo R, Marquez M, Ganan-Calvo AM. Micro/nano encapsutation via electrified coaxial liquid jets. *Science* 2002;**295**:1695–8.
16. Cloupeau M, Prunet-Foch B. Electrohydrodynamic spraying functioning modes: a critical review. *J Electrostat* 1994;**25**:1021–36.
17. Chen QZ, Zhang HB, Wang DZ, Edirisinghe MJ, Boccaccini AR. Improved mechanical reliability of bone tissue engineering (zirconia) scaffolds by electrospraying. *J Am Ceram Soc* 2006;**89**:1534–9.
18. Jayasinghe SN, Edirisinghe MJ. Novel forming of single and multiple ceramic micro-channels. *Appl Phys A: Mater* 2005;**80**:701–2.
19. Dauchy F, Dorey RA. Patterned crack-free PZT films for micro-electromechanical system applications. *In J Adv Manuf Technol* 2007;**33**:86–94.
20. Jayasinghe SN, Edirisinghe MJ, Wang DZ. Controlled deposition of nanoparticleclusters by electrohydrodynamic atomization. *Nanotechnology* 2004;**15**:1519–23.
21. Wang D, Rocks SA, Dorey RA. Formation of PZT micro-scale structures using electrohydrodynamic atomization filling of metallic moulds. *J Eur Ceram Soc* 2010;**30**:1821–6.
22. Sun D, Rocks SA, Edirisinghe MJ, Dorey RA, Wang Y. Electrohydrodynamic deposition of nanostructured Lead Zirconate Titanate. *J Nanosci Nanotechnol* 2005;**5**:1846–51.
23. Dorey RA, Stringfellow SB, Whatmore RW. Effect of sintering aid and repeated sol infiltrations on the dielectric and piezoelectric properties of a PZT composite thick film. *J Eur Ceram Soc* 2002;**22**:2921–6.
24. Villegas M, Moure C, Jurado JR, Duran P. Improvements of sintering and piezoelectric properties of soft lead zirconate titanate ceramics. *J Mater Sci* 1994;**29**:4975–83.
25. Barrow DA, Petroff TE, Sayer M. Thick ceramic coatings using a sol–gel based ceramic 0–3 composite. *Surf Coat Technol* 1995;**76–77**:113–8.
26. Wang D, Edirisinghe MJ, Dorey RA. Formation of PZT crack-free thick films by electrohydrodynamic atomization deposition. *J Eur Ceram Soc* 2008;**28**:2739–45.
27. Dorey RA, Whatmore RW. Electrical properties of high density PZT and PMN-PT/PZT thick films produced using ComFi technology. *J Eur Ceram Soc* 2004;**24**:1091–4.
28. Bowen CR, Kara H. Pore anisotropy in 3–3 piezoelectric composites. *Mater Chem Phys* 2002;**75**:45–9.
29. Nye JF. *Physical properties of crystals*. Oxford: Oxford University Press; 1957.
30. Dorey RA, Whatmore RW, Beeby SP, Torah RN, White NM. Screen printed PZT composite thick films. *Integr Ferroelectr* 2004;**63**:601–4.
31. Bardaine A, Boy P, Belleville P, Acher O, Levassort F. Improvement of composite sol–gel process for manufacturing 40 μm piezoelectric thick films. *J Eur Ceram Soc* 2008;**28**:1649–55.
32. Lee SG. Effects of sol infiltration on the screen-printed lead zirconate titanate thick films. *Mater Lett* 2007;**61**:1982–5.
33. Wang ZH, Miao JM, Zhu WG. Piezoelectric thick films and their application in MEMS. *J Eur Ceram Soc* 2007;**27**:3759–64.